Discrepancy of mass transport between the Northern and Southern Hemispheres among the ERA-40, NCEP/NCAR, NCEP-DOE AMIP-2, and JRA-25 reanalysis

Yufei Zhao[1,2] and Jianping Li[3]

Received 20 June 2006; revised 17 August 2006; accepted 7 September 2006; published 20 October 2006.

[1] The atmospheric mass transfer between the Northern Hemisphere (NH) and the Southern Hemisphere (SH) across the equator is calculated from the ERA-40, the NCEP/NCAR (NCEP 1), the NCEP-DOE AMIP-2 (NCEP 2) and the Japanese 25-year Reanalysis (JRA-25) and explored for trends which have some notable differences, even contrary phase in the mean annual cycle. The hemispheric and global mean surface pressure anomalies have the coincident trends for the four datasets. The varieties of mass flux and mean surface pressure anomalies are comparatively coincident in ERA-40 and JRA-25 (when the mass flux is northerly (southerly), the mean surface pressure in NH increases (decreases)), but almost contrary verdict in NCEP 1. There's been a notable improvement in NCEP 2 upon NCEP 1, however, NCEP 2 seems likely still not as good as ERA-40 and JRA-25. Furthermore, the research also expands to 60°S–60°N.
Citation: Zhao, Y., and J. Li (2006), Discrepancy of mass transport between the Northern and Southern Hemispheres among the ERA-40, NCEP/NCAR, NCEP-DOE AMIP-2, and JRA-25 reanalysis, *Geophys. Res. Lett.*, *33*, L20804, doi:10.1029/2006GL027287.

1. Introduction

[2] The monitoring of climate, the validation of atmospheric models, and the understanding of physical processes all require accurate, dynamically consistent analyses of the available observations [*Pawson and Fiorino*, 1998a, 1998b, 1998c]. In the recent years, several reanalyses of many global meteorological fields are widely used. These involve the National Center for Environmental Prediction-National Center for Atmospheric Research (NCEP-NCAR) reanalysis from the late 1940s to present [*Kalnay et al.*, 1996], the NCEP-DOE Atmospheric Model Intercomparison Project (AMIP-2) reanalysis covering 1979-present [*Kanamitsu et al.*, 2002] which includes several improvements in the assimilation scheme, is nearly identical to that of the earlier NCEP 1 [*Hines et al.*, 2000], the European Centre for Medium-Range Weather Forecasts reanalysis from mid-1957 to mid-2002 [*Uppala et al.*, 2005] and so on. And recently the Japanese 25-year reanalysis has been released for general use [*Onogi et al.*, 2005] (also K. Onogi et al., The JRA-25 Reanalysis, submitted to *Journal of Meteorological Society of Japan*, 2006). The total mass of the atmosphere is usually measured by the global and hemispheric mean surface pressure [e.g., *Trenberth*, 1981; *Trenberth et al.*, 1987; *Chen et al.*, 1997; *Hoinka*, 1998]. This study employs not only the averaged surface pressure but the whole mass flux to describe the annual cycle of the hemispheric and global atmospheric mass, and moreover, considers the four reanalyses from the angle of the mass flux of global scale and hemispherical scale and it could likely provide some references to the further work and the evaluation of models.

[3] The global mass of the atmosphere is approximately conserved [*Trenberth et al.*, 2005]. Global surface pressure, which represents the total mass of the atmosphere, exhibits an annual cycle, with a maximum during the boreal summer [*Trenberth*, 1981]. Therefore, there are net mass transportations between NH and SH, and that will result in the varieties of the mean surface pressure of the hemisphere consequentially.

[4] The net mass flux of whole layer at p coordinate is stated as [*Zeng and Li*, 2002]

$$I = \frac{1}{g}\int_0^{ps} v\mathrm{d}p \tag{1}$$

where p_s is the surface pressure and v is the meridional wind and g = 9.80665 m s^{-2} is the gravity acceleration. In the material calculations, this paper assumes that the meridional wind, i.e. mass flux below the ground is zero and the top level is 10 hPa just because these four kinds of reanalyses all have the same top level of 10 hPa. Let $[\bar{I}]$ be the zonal climatological mean of (1). Monthly mean surface pressure and meridional wind data are used. These variables have a regular resolution of 2.5° latitude and 2.5° longitude except for ERA-40 surface pressure data, which is on N80 reduced Gaussian grid. Computations are based on monthly mean data for the whole year in 1979–2001, except for JRA-25 in 1979–2000.

2. Results

[5] Figure 1 shows the annual cycle of the whole mass flux $[\bar{I}]$, which has several features of interest. Remarkably, the first is the considerable offset among the four estimates of mass transfer across the equator. The second feature is the almost reverse annual cycle phase for ERA-40 and NCEP 1 which highlights striking differences between them con-

[1]College of Atmospheric Sciences, Lanzhou University, Lanzhou, China.
[2]Now at State Key Laboratory of Numerical Modelling for Atmospheric Sciences and Geophysical Fluid dynamics (LASG), Institute of Atmospheric Physics, Chinese Academy of Sciences, Beijing, China.
[3]State Key Laboratory of Numerical Modelling for Atmospheric Sciences and Geophysical Fluid dynamics (LASG), Institute of Atmospheric Physics, Chinese Academy of Sciences, Beijing, China.

0094-8276/06/2006GL027287$05.00

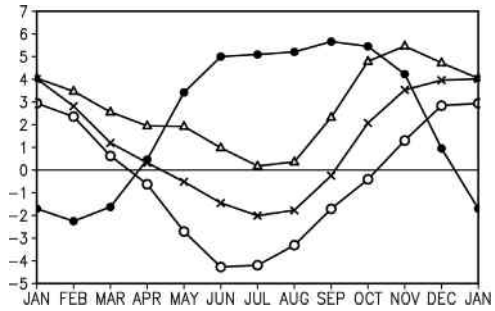

Figure 1. Annual cycle of the whole mass flux $[\bar{I}]$ (10^2 kg m^{-1} s^{-1}) at the equator for ERA-40 (open circle line), NCEP 1 (closed circle line), NCEP 2 (open triangle line) and JRA-25 (multiplication sign line).

cerning the interhemispheric mass exchange. The annual mean mass flux at the equator is estimated to be -0.5969×10^2 kg m^{-1} s^{-1} for ERA-40, 2.4902×10^2 kg m^{-1} s^{-1} for NCEP 1, 2.7290×10^2 kg m^{-1} s^{-1} for NCEP 2 and 0.9926×10^2 kg m^{-1} s^{-1} for JRA-25, respectively. From the above quantities, it could be apparent that there are distinct differences among the four reanalyses, especially ERA-40 from NCEP 1 and NCEP 2.

[6] Surface pressure is a reliable indicator of the whole atmospheric mass. Moreover, it is one of the easier measurements to make accurately and a representative quantity in the atmosphere. Table 1 shows the global, NH, SH and SH minus NH (SH-NH) annual mean surface pressure from ERA-40, NCEP 1, NCEP 2 and JRA-25. It could be seen that the surface pressure difference of SH-NH is 451.39, 522.83, 553.14 and 467.09 hPa for ERA-40, NCEP 1, NCEP 2 and JRA-25, i.e., the pressures of NCEP 1, NCEP 2 and JRA-25 are higher than that of ERA-40 for 15.83%, 22.54% and 3.48%, respectively. Global surface pressure has an annual cycle of 0.25 hPa (Figure 2a) for ERA-40, 0.40 hPa for NCEP 1 (Figure 2b), 0.42 hPa for NCEP 2 (Figure 2c) and 0.32 hPa for JRA-25 (Figure 2d), all with a maximum during the boreal summer. It shows that the highest surface pressure occurs in the winter hemisphere. From Figure 2 it could be seen that the air always flows from NH to SH across the equator in the boreal summer and flows from SH to NH in winter. Since we expect that the atmospheric mass is truly a constant, the departures from zero give an exact measure of the magnitude of the mean annual cycle of vapor pressure and the errors in P_s [*Trenberth and Smith*, 2005]. The difference of mean annual cycle of the hemispheric and global mean surface pressure anomalies for p_s is very small for NCEP 1 and NCEP 2. And the relative prominent unlikeness of the three curves (NH, SH and GL) for these four datasets occurs in the NH curve of boreal winter which shows almost twice value in ERA-40 than the other three. Though there are some distinctions in the four outcomes, the SH curve is comparatively higher and NH lower in May–June–July–August–September, and the SH curve is lower and NH higher in the other months, i.e., the seasonal migration of air is southward across the equator in May–September, and northward in October–April. However the mass flux (Figure 1) has great distinctions for the four reanalyses, even opposite phase variety between ERA-40 and NCEP 1 in some months. When the mass flux is northerly (southerly) over the equator, the mean surface pressure in NH is supposed to

Table 1. Global (GL), NH, SH and SH-NH Annual Mean Surface Pressure From ERA-40, NCEP 1, NCEP 2 and JRA-25[a]

	ERA-40	NCEP 1	NCEP 2	JRA-25
GL	98545.82	98490.42	98467.52	98536.21
NH	98320.12	98229.00	98199.95	98302.66
SH	98771.51	98751.83	98753.09	98769.75
SH-NH	451.39	522.83	553.14	467.09

[a]Unit: hPa.

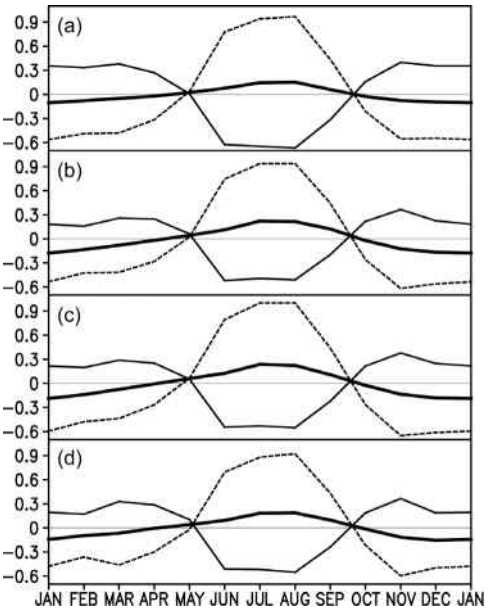

Figure 2. Annual variation in the average surface pressure (in hPa) over the NH (thin solid line), SH (dashed line) and the globe (thick solid line) for (a) ERA-40, (b) NCEP 1, (c) NCEP 2 and (d) JRA-25 reanalysis. Plotted are departures from the annual mean values.

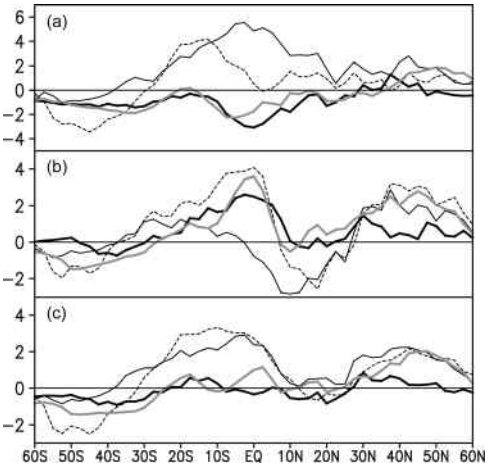

Figure 3. Meridional profiles of the zonally-mean mass flux $[\bar{I}]$ (10^2 kg m^{-1} s^{-1}) from ERA-40 (heavy solid line), NCEP 1 (thin solid line), NCEP 2 (dashed line) and JRA-25 (heavy grey solid line) for (a) JJA, (b) DJF and (c) annual mean conditions.

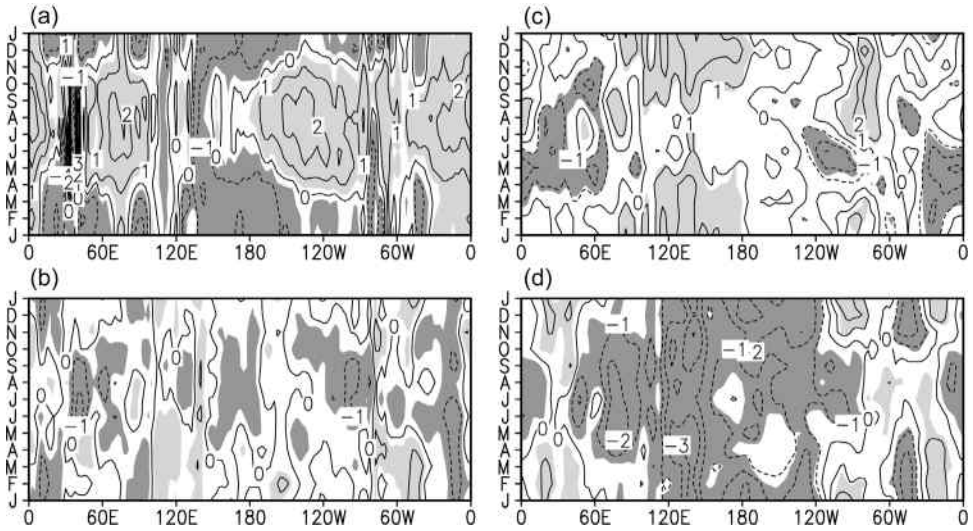

Figure 4. The annual cycle of the mean meridional wind (m s^{-1}) that is educed by subtracting the value of NCEP 1 from ERA-40 at the equator for (a) 850 hPa, (b) 500 hPa, (c) 200 hPa and (d) 100 hPa. The contour interval is 1 m s^{-1}. The shaded areas denote where the differences are significant at 95% confidence level according to the Student's *t*-test.

increase (decrease). Contrasting Figures 1 and 2, it shows that the mass flux and surface pressure are consistent in ERA-40 and JRA-25 but NCEP 1 has some spurious signals in meridional wind at the equator, and the quality of that for NCEP 2 appears somewhat ameliorative.

3. Further Analysis

[7] Further research has done to inspect the specifics such as whether it is a separate case at the equator, Figure 3 shows the whole mass transport $[\overline{I}]$ within 60°S–60°N (just because of the likely inaccurate information in the residual latitudes of 90°S–60°S and 60°N–90°N).

[8] Figure 3 illustrates that $[\overline{I}]$ varies gently and has positive or negative mass transport in different latitude circles for ERA-40, NCEP 1, NCEP 2 and JRA-25 either in summer, winter or annually mean conditions. It can be seen that the differences of mass advection for these reanalyses are notable not only in the equator but also from 60°S to 60°N. Essentially, the annually mean net transport between every two latitude circles should verge on zero to ensure the stability of the global system in sense of climatological average. Figure 3 shows that for JRA-25, especially for ERA-40 the annually mean $[\overline{I}]$ is smaller than for NCEP 1 and NCEP 2, i.e., the JRA-25 and ERA-40 might accord with the above verdict better and best, respectively. The annual mean $[\overline{I}]$ might be mainly caused by the changes in precipitation and evaporation, ejecting of volcanoes and so on. The major latitude ranges of mass exchange are in the tropics, and the whole mass flux is also considerable for the four data sets in summer and winter in 30°–50°N.

[9] The essential problems of different mass transport over the latitude circles proceed from the distinctions of meridional wind for dissimilar reanalyses. Figures 4–6 present three latitude-month plots of the zonally averaged

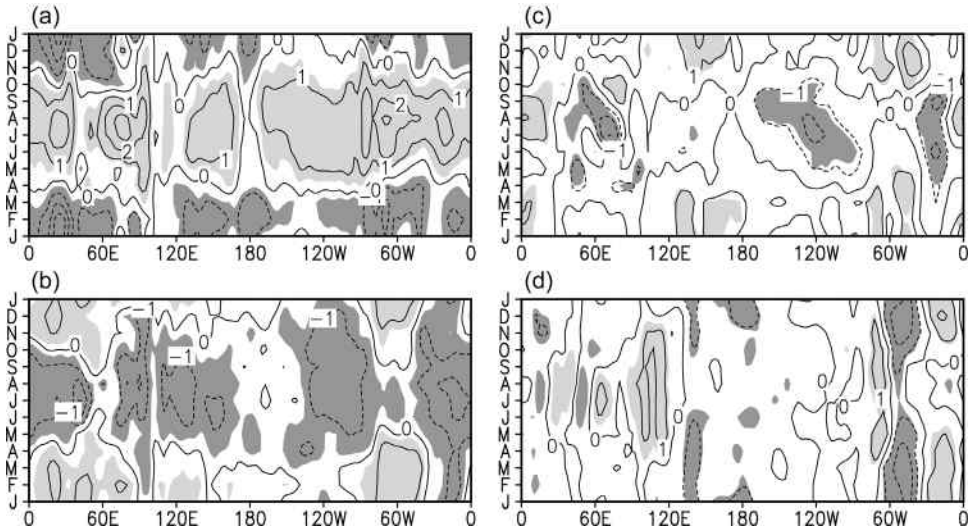

Figure 5. Same as Figure 4 but subtracting NCEP 1 from NCEP 2.

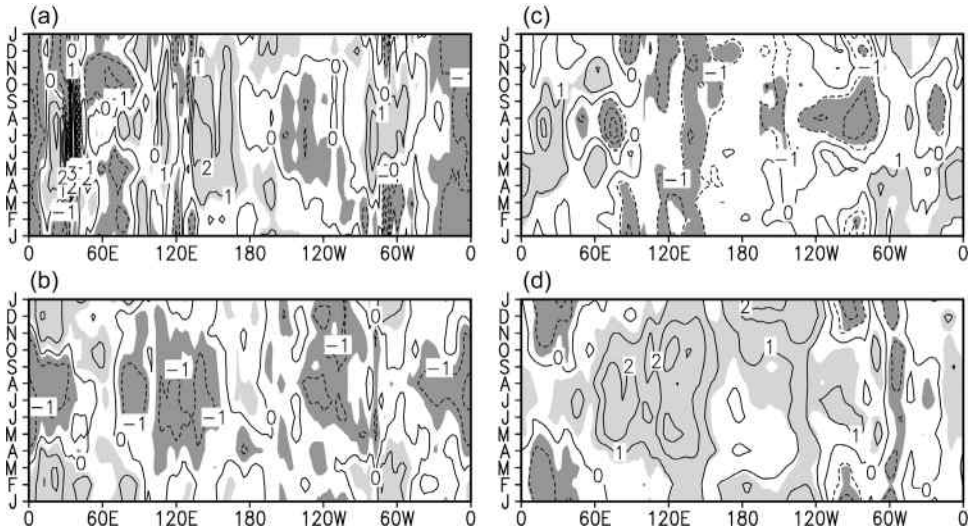

Figure 6. Same as Figure 4 but subtracting ERA-40 from NCEP 2.

difference of meridional wind at the equator and the significant regions (at 95% confidence level) for ERA-40 minus NCEP 1, NCEP 2 minus NCEP 1 and NCEP 2 minus ERA-40, respectively, in turn on the pressure levels of 850 hPa, 500 hPa, 200 hPa and 100 hPa. For the limit of length, all the levels (17 levels) will not be shown. The difference between ERA-40 and NCEP 1 is the largest one while concerning either the wind speed or the magnitude of significant regions. Except the several top levels (from 70 hPa to10 hPa), the other layers have maximum significant regions.

[10] Figure 4 shows that ERA-40 departs NCEP 1 comparatively even more far in the lower troposphere (850 hPa) and the stratosphere (100 hPa) than in the middle troposphere (500 hPa) and the upper troposphere (200 hPa). In the level of 850 hPa, the extrema occur in summer and winter the whole equatorial circle approximately. Apparently, different pressure levels have different longitudes at which the value is maximum or minimum. In general, the dissimilarities between the two reanalyses consist in the all year and the whole equatorial circumference. Figure 5 presents the meridional wind of NCEP 2 minus NCEP 1. At the lower and middle troposphere the differences are more remarkable than the other two levels, i.e., there might be some obvious amendments in the meridional velocity field, especially at the lower and middle troposphere for NCEP 2 at the equator. The results of subtracting ERA-40 from NCEP 2 are shown in Figure 6. Generally, the differences between these two datasets are less remarkable than those between NCEP 1 and ERA-40. The difference between ERA-40 and JRA-25 is the most inconspicuous one (not shown).

4. Summary and Discussion

[11] The comparison result among ERA-40, NCEP-NCAR, NCEP-DOE AMIP-2 and JRA-25 reanalysis in this paper shows clear evidence that there are significant distinctions in the atmospheric mass flux between NH and SH among these four datasets. The constraint relationship between the atmospheric mass transfer and surface pressure is used in the analyses. Overall, when the mass flux is northerly (southerly) over the equator, the mean surface pressure in NH increases (decreases) in both ERA-40 and JRA-25, satisfying the constraint above. However, the trends of the surface pressure and mass flux in NCEP 1 might conflict with each other to a great extent. Furthermore, not only at the equator, the research is also expanded to the latitudes from 60°S to 60°N. The difference among the four datasets are also notable. The output of ERA-40 might be more rational. On the one hand, the mass flux across the equator and the mean surface pressure are consistent in ERA-40. On the other hand, the annually mean net transport between every two latitude circles should verge on zero to ensure the stability of the global system in sense of climatological average, and for ERA-40 the annually mean $[\bar{I}]$ is the smallest one, i.e., the ERA-40 might accord with the above verdict best. The result of JRA-25 also reflects the verdict better. The spurious trends in the meridional wind might exist in ERA-40, NCEP 1, NCEP 2 and JRA-25, especially in NCEP 1, and comparing with NCEP 1 the trends are improved in NCEP 2 to a certain extent. The causes for the discrepancy among these four reanalyses might be the different assimilation and parameterization procedures they adopt. Some cautions should be given while considering the mass flux for the four reanalyses.

[12] **Acknowledgments.** Thanks are owed to two anonymous reviewers for their helpful comments. This work was supported jointly by NSFC Projects (40325015, 40523001) and CAS International Partnership Creative Group (The Climate System Model Development and Application Studies).

References

Chen, T. C., et al. (1997), Seasonal variation of global surface pressure and water vapor, *Tellus, Ser. A*, *49*, 613–621.

Hines, K. M., D. H. Bromwich, and G. J. Marshall (2000), Artificial surface pressure trends in the NCEP-NCAR Reanalysis over the southern ocean and Antarctica, *J. Clim.*, *13*, 3940–3952.

Hoinka, K. P. (1998), Mean global surface pressure series evaluated from ECMWF reanalysis data, *Q. J. R. Meteorol. Soc.*, *124*, 2291–2297.

Kalnay, E., et al. (1996), The NCEP/NCAR 40-year reanalysis project, *Bull. Am. Meteorol. Soc.*, *77*, 437–471.

Kanamitsu, M., et al. (2002), NCEP-DOE AMIP-II Reanalysis (R-2), *Bull. Am. Meteorol. Soc.*, *83*, 1631–1643.

Onogi, K., et al. (2005), JRA-25: Japanese 25-year re-analysis project—Progress and status, *Q. J. R. Meteorol. Soc.*, *131*, 3259–3268.

Pawson, S., and M. Fiorino (1998a), A comparison of reanalyses in the tropical stratosphere: Part 1. Thermal structure and the annual cycle, *Clim. Dyn.*, *14*, 631–644.

Pawson, S., and M. Fiorino (1998b), A comparison of reanalyses in the lower tropical stratosphere: Part 2. The quasi-biennial oscillation, *Clim. Dyn.*, *14*, 645–658.

Pawson, S., and M. Fiorino (1998c), A comparison of reanalyses in the lower tropical stratosphere: Part 3. Inclusion of the pre-satellite data era, *Clim. Dyn.*, *15*, 241–250.

Trenberth, K. E. (1981), Seasonal variations in global sea level pressure and the total mass of the atmosphere, *J. Geophys. Res.*, *86*, 5238–5246.

Trenberth, K. E., and L. Smith (2005), The mass of the atmosphere: A constraint on global analyses, *J. Clim.*, *18*, 864–875.

Trenberth, K. E., J. R. Christy, and J. G. Olson (1987), Global atmospheric mass, surface pressure, and water vapor variations, *J. Geophys. Res.*, *92*, 14,815–14,826.

Trenberth, K. E., D. P. Stepaniak, and L. Smith (2005), Interannual variability of patterns of atmospheric mass distribution, *J. Clim.*, *18*, 2812–2825.

Uppala, S. M., et al. (2005), The ERA-40 re-analysis, *Q. J. R. Meteorol. Soc.*, *612*, 2961–3012.

Zeng, Q., and J. Li (2002), Interactions between the Northern and Southern Hemispheric atmospheres and the essence of monsoon, *Chin. J. Atmos. Sci.*, *26*(3), 207–226.

J. Li and Y. Zhao, State Key Laboratory of Numerical Modelling for Atmospheric Sciences and Geophysical Fluid dynamics (LASG), Institute of Atmospheric Physics, Chinese Academy of Sciences, Beijing 100029, China. (ljp@lasg.iap.ac.cn; zyf@mail.iap.ac.cn)